Enhanced DCT-OFDM System With Index Modulation

Chang He, Aijun Cao, Lixia Xiao, Lei Zhang, Pei Xiao and Konstantinos Nikitopoulos

***Abstract*—Discrete cosine transform (DCT) based orthogonal frequency division multiplexing (OFDM), which has double number of subcarrier compared to the classic discrete fourier transform (DFT) based OFDM (DFT-OFDM) at the same bandwidth, is a promising high spectral efficiency multicarrier techniques for future wireless communication. In this paper, an enhanced DCT-OFDM with index modulation (IM) (EDCT-OFDM-IM) is proposed to further exploit the benefits of the DCT-OFDM and IM techniques. To be more specific, a pre-filtering method based DCT-OFDM-IM transmitter is first designed and the non-linear maximum likelihood (ML) is developed for our EDCT-OFDM-IM system. Moreover, the average bit error probability (ABEP) of the proposed EDCT-OFDM-IM system is derived, which is confirmed by our simulation results. Both simulation and theoretical results are shown that the proposed EDCT-OFDM-IM system exhibits better bit error rate (BER) performance over the conventional DFT-OFDM-IM and DCT-OFDM-IM counterparts.**

***Index Terms*—Discrete cosine transform (DCT), index modulation (IM), performance analysis.**

I. Introduction

Orthogonal frequency division multiplexing (OFDM) with index modulation (IM) (OFDM-IM), which employs the activated subcarrier indices as an additional means of implicitly conveying information, has been regarded as a promising OFDM variant. In the OFDM-IM scheme, parts of the subcarriers are activated to modulate the corresponding data symbols while the rest subcarriers are idle for data transmission [1], [2], [3]. Therefore, the OFDM-IM exhibits better bit error ratio (BER) as well as peak-to-average power ratio (PAPR) performance over its classic OFDM counterpart [4], [5], [6] with low modulation order. Recent studies have been shown that the OFDM-IM scheme is a promising candidate for Vehicle-to-Vehicle (V2V) or Vehicle-to-Infrastructure (V2X) [7], [8], as well as 5G and beyond wireless communication scenarios.

However, the existing OFDM-IM schemes are mainly implemented based on the classic OFDM structures, where the discrete Fourier transform (DFT) pair are employed as multiplexing/de-multiplexing operations. In fact, there exists another multicarrier scheme using a cosinusoidal set as an orthogonal basis, which can be implemented with the discrete cosine transform (DCT) pair modules [9]. For convenience, we term this system as DCT-OFDM, while the classic OFDM system is termed as DFT-OFDM in this paper. By using the DCT pair, many appealing benefits for the DCT-OFDM system implementation are verified. Firstly, the fast DCT algorithm of [10], could reduce the computation complexity of the fast Fourier transform (FFT) algorithms in DFT-OFDM system. Secondly, the excellent energy concentration and spectral compaction properties inherited by DCT render the DCT-OFDM system more robust against the inter carrier interference (ICI) effect [11]. Furthermore, since only half of the minimum subcarrier spacing is required to guarantee its subcarrier orthogonality [12], the total number of subcarriers in the DCT-OFDM system is doubled compared to the classic DFT-OFDM system. Due to these advantages, the DCT-OFDM constitutes a promising and highly spectrally multicarrier techniques for future wireless communication.

In order to exploit the benefits of the DCT-OFDM and IM schemes, the DCT-OFDM-IM was first proposed by Marwa in [14], which has demonstrated that it is capable of achieving significant spectrum efficiency (SE) gains over its DFT-OFDM-IM counterpart. However, the original DCT-OFDM-IM scheme was implemented by cyclic prefix (CP) assisted transceiver structure and linear detection based receiver, the research on DCT-OFDM-IM is still in its infancy and there is a lot of room for further performance improvement.

Against the above background, the contributions of this paper are summarized as follows:

1) A pre-filtering approach based enhanced DCT-OFDM-IM (EDCT-OFDM-IM) is proposed, where instead of CP the prefix and suffix are added to avoid the inter symbol interference (ISI) and ICI. More specifically, the prefix and suffix are inserted as symmetric extension from the information sequences at both sides of a transmitted sequence block.
2) Both linear detector and the maximum likelihood (ML) detector are presented for our proposed EDCT-OFDM-IM system. Simulation results show that the ML based EDCT-OFDM-IM system is capable of providing significant performance gain over the linear detector based DCT-OFDM-IM system [14].
3) The upper bound of the Average Bit Error Probability (ABEP) of our proposed EDCT-OFDM-IM system is derived. Furthermore, the advantages of the EDC-OFDM-IM system are also evaluated by minimum Euclidean distance (MED). Both theoretical and simulation results are demonstrated and shown that our proposed EDCT-OFDM-IM is more robust against the frequency offset

C. He, A. Cao, L. Xiao, P. Xiao and K. Nikitopoulos are with 5G Innovation Centre (5GIC), University of Surrey, Guildford, UK. L. Zhang is with Glasgow College UESTC, University of Glasgow, UK.

L. Xiao is also with the Wuhan National Laboratory for Optoelectronics, School of Electronic Information and Communications, Huazhong University of Science and Technology. The corresponding author is Lixia Xiao. (Email:{l.xiao}@surrey.ac.uk).

This work was supported in part by the U.K. Engineering and Physical Sciences Research Council under Grant EP/R001588/1 and EP/S02476X/1. The authors also would like to acknowledge the support of the University of Surrey 5GIC.

than DFT-OFDM-IM.

Notations: The dimension $N\times N$ matrix $\mathbf{I}_N$, $\mathbf{J}_N$ and $\mathbf{0}_{M\times N}$, are the identity matrix, reversal matrix and zero matrix, respectively. (L, K, N) denotes a IM scheme where K subcarriers are activated within a group of L subcarriers, and N is the total number of available subcarriers.

II. Proposed EDCT-OFDM-IM system model

The major limitation of the DCT-OFDM is that, the circular convolution property which is always satisfied by DFT does not hold for DCT [9], [15]. To address this issue and to further improve the performance of DCT-OFDM-IM, we follow the implementation of an enhanced DCT-OFDM transceiver structure based on the pre-filtering method in [11], [12].

A. Transceiver Structure

Consider an EDCT-OFDM-IM system employs N subcarriers, and the total subcarriers are separated into G groups with each consisting of $L = N/G$ subcarriers. We denote each group by $\mathbf{Y}_g = [Y_{(g,0)}, Y_{(g,1)}, \ldots, Y_{(g,L-1)}]^T$, $g = 0, 1, \ldots, G-1$. Then the data symbol vector can be given as:

$$\hat{\mathbf{x}} = [\mathbf{Y}_0^T, \mathbf{Y}_1^T, \ldots, \mathbf{Y}_{G-1}^T]^T. \tag{1}$$

For each group, K out of L available subcarriers are activated to map $p_1 = \lfloor \log_2 C_L^K \rfloor$ bits into a set of subcarrier indices combinations. On the other hand, $p_2 = K\log_2(M)$ bits are modulated to M-ary ASK data symbols and subsequently transmitted by the K active subcarriers. Accordingly, the total number of bits transmitted per EDCT-OFDM-IM block is $G\cdot(p_1+p_2) = Gp$. After subcarrier IM, the g-th group signal can be written as

$$\mathbf{Y}_g = [0, \ldots, s_{(g,0)}, 0, \ldots, s_{(g,1)}, 0, \ldots, s_{(g,K-1)}, 0, \ldots]^T, \tag{2}$$

where $s_{(g,k)} (k = 0, 1, \ldots, K-1)$ represents the M-ary ASK constellation point, and $\mathbf{Y}_g \in \Lambda$, where Λ is the set of all possible symbol vector combinations. After subcarrier level block interleaving, the modified transmitted signals can be expressed as

$$\begin{aligned}\mathbf{x} &= [X_0, X_1, \ldots, X_{N-1}] \\ &= [Y_{(0,0)}, Y_{(1,0)}, \ldots, Y_{(G-1,0)}, \ldots, Y_{(0,L-1)}, Y_{(1,L-1)}, \ldots, Y_{(G-1,L-1)}].\end{aligned} \tag{3}$$

In general, the symmetric extended prefix and suffix are assumed to have the same length v. Therefore, the total block length is $L_1 = N + 2v$ and the transmitted signal vector is represented by

$$\mathbf{u} = \mathbf{T}_{PS}\mathbf{D}^H\mathbf{x}, \tag{4}$$

where $\mathbf{D} \in \mathbb{R}^{N\times N}$ is a power normalised type-II DCT matrix with its (l, m) entry given by:

$$d_{l,m} = \begin{cases} \sqrt{\frac{2}{N}}\cos(\frac{(l-1)(2m-1)\pi}{2N}), & l > 1 \\ \sqrt{\frac{1}{N}}, & l = 1. \end{cases} \tag{5}$$

$\mathbf{T}_{PS} = [\mathbf{J}_v, \mathbf{0}_{v\times(N-v)}; \mathbf{I}_N; \mathbf{0}_{v\times(N-v)}, \mathbf{J}_v]$ is the $L_1 \times N$ matrix that inserts the prefix and suffix at both sides of a data symbol block.

Assume a Rayleigh fading channel vector at L_c taps in the time domain as defined by $\mathbf{h} = [h_0, h_1, \ldots, h_{L_c-1}]$. Its corresponding time-reverse pre-filter vector is thus in the reverse form as $\mathbf{p} = [h_{L_c-1}, h_{L_c-2}, \ldots, h_0]$. Correspondingly, the matrix form of the multipath channel $\mathbf{H} \in \mathbb{R}^{L_1\times L_1}$ is represented as a Toeplitz matrix with its first row and first column being $[h_{L_c-1}, h_{L_c-2}, \ldots, h_0, \mathbf{0}_{1\times(L_1-L)}]$ and $[h_{L_c-1}, \mathbf{0}_{1\times(L_1-1)}]^T$ respectively, while the matrix form of the pre-filter $\mathbf{P} \in \mathbb{R}^{L_1\times L_1}$ is represented also by a Toeplitz matrix with its first row and column being $[h_{L_c-1}, \mathbf{0}_{1\times(L_1-1)}]$ and $[h_{L_c-1}, h_{L_c-2}, \ldots, h_0, \mathbf{0}_{1\times(L_1-L)}]^T$, respectively.

At the receiver side, by performing the time-reverse pre-filtering and the DCT demultiplexing, the received frequency-domain sample vector obtained after guard sequence removal can be expressed as

$$\mathbf{z} = \mathbf{D}\mathbf{R}_{PS}\mathbf{P}(\mathbf{H}\mathbf{u} + \mathbf{n}), \tag{6}$$

The guard sequence removal operation is denoted by the matrix $\mathbf{R}_{PS} = [\mathbf{0}_{N\times v}, \mathbf{I}_N, \mathbf{0}_{N\times v}]$. $\mathbf{n} \in \mathbb{R}^{L_1\times 1}$ is the Additive white Gaussian noise (AWGN) noise vector with its elements subject to Gaussian distribution with zero mean and N_0 variance.

Recalling the aforementioned one-tap equalization mechanism, with the introduction of a pre-filter and the symmetric guard sequence, the EDCT-OFDM-IM is now applicable for ICI and ISI free transmission. This integrates the output of $\mathbf{D}\mathbf{R}_{PS}\mathbf{P}\mathbf{H}\mathbf{T}_{PS}\mathbf{D}^H$ equivalent to an effective diagonal matrix $\mathbf{H}_{eff}$ and (6) thus can be simplified to

$$\mathbf{z} = \mathbf{H}_{eff}\mathbf{x} + \mathbf{G}_{eff}\mathbf{n} \tag{7}$$

where $\mathbf{H}_{eff} \in \mathbb{R}^{N\times N}$ is the effective channel diagonal matrix with its elements expressed by $diag(\mathbf{H}_{eff}) = [H_0, H_1, \ldots, H_{N-1}]$, and $\mathbf{G}_{eff} = \mathbf{D}\mathbf{R}_{PS}\mathbf{P}$ represents the effective noise correlation matrix.

B. Proposed ML detector

Due to the correlated pre-filtering procedure, the noise vector becomes correlated and subject to different kinds of correlation gains. In order to calculate the effective noise variance for each subcarrier, we take a scaled form from (7), as expressed by

$$Z_k = H_k X_k + \sum_{i=1}^{N} g_{k,i} n_i \tag{8}$$

where Z_k and n_i are the received sample and AWGN sample at the kth subcarrier and ith subcarrier, respectively, whereas $g_{k,i}$ is the entry in the kth row and ith column of $\mathbf{G}_{eff}$.

We make a reasonable assumption that time is long over symbols. With this assumption, $g_{k,i}^2$ is regarded as instant noise coefficient and the overall coloured noise coefficient on arbitrary subcarrier index is in the summation of the noise coefficient from all subcarriers. Accordingly, the coloured noise variance V_k at subcarrier index k can be obtained as

$$V_k = \frac{N_0}{2}\sum_{i=1}^{N} g_{k,i}^2 \quad . \tag{9}$$

Based on the instantaneous coloured noise variance V_k, we reformulated the expression of the optimum ML detection for gth group. Denoting by $Z_{g+\lambda G} = Z_{(g,\lambda)}$, $H_{g+\lambda G} = H_{(g,\lambda)}$ and $V_{g+\lambda G} = V_{(g,\lambda)}$, the transmit symbols in the gth group can be estimated as

$$\hat{\mathbf{Y}}_g = \underset{\mathbf{Y}_g\in\Lambda}{\arg\min} \sum_{\lambda=0}^{L-1} \frac{|Z_{(g,\lambda)} - H_{(g,\lambda)}Y_{(g,\lambda)}|^2}{V_{(g,\lambda)}}. \tag{10}$$

TABLE I
MED COMPARISONS UNDER THE SAME BANDWIDTH

SE	Modulation Scheme	MED^t	MED^p
1bits/s/Hz	EDCT-OFDM-IM (8,1,128) BPSK	16	10.72
	DFT-OFDM-IM (4,1,64) 4QAM	8	4.48
	DFT-OFDM (4,4,64) BPSK	4	2.24
1.5bits/s/Hz	EDCT-OFDM-IM (4,1,128) BPSK	8	5.36
	DFT-OFDM-IM (2,1,64) 4QAM	4	2.24
	EDCT-OFDM-IM (8,2,128) BPSK	8	5.88
	DFT-OFDM-IM (4,2,64) 4QAM	4	2.52
2bits/s/Hz	EDCT-OFDM-IM (8,3,128) BPSK	5.33	4.08
	DFT-OFDM-IM (4,3,64) 4QAM	2.67	2.053
	DFT-OFDM (4,4,64) 4QAM	2	1.54

As indicated in (10), the noise correlation effect can be effectively compensated by the term $V_{g+\lambda G}$.

III. Performance Analysis For The Proposed EDCT-OFDM-IM

A. ABEP Analysis of the EDCT-OFDM-IM

For the EDCT-OFDM-IM scheme, let $(\mathbf{Y}_g \rightarrow \tilde{\mathbf{Y}}_g, \mathbf{H}_g)$ denotes the pair wise error event where the transmitted signal $\mathbf{Y}_g$ in the g-th group is erroneously detected as $\tilde{\mathbf{Y}}_g$ conditioned on the corresponding effective channel coefficient vector $\mathbf{H}_g$. In this regard, the conditional PEP (CPEP) expression in [16], can be reformulated by compensating the coloured noise variance $V_{(g,\lambda)}$ on each subcarrier, and is expressed as

$$P(\mathbf{Y}_g \rightarrow \tilde{\mathbf{Y}}_g, \mathbf{H}_g) = Q(\sqrt{\delta}) \approx \frac{1}{12}e^{-\delta/2} + \frac{1}{4}e^{-2\delta/3} \quad (11)$$

where

$$\delta = \sum_{\lambda=0}^{L-1} \frac{|H_{(g,\lambda)}Y_{(g,\lambda)} - H_{(g,\lambda)}\tilde{Y}_{(g,\lambda)}|^2}{2V_{(g,\lambda)}} \quad (12)$$

The unconditional PEP (UPEP), is thus obtained by taking the average of the effective channel coefficients of the CPEP as

$$P(\mathbf{Y}_g \rightarrow \tilde{\mathbf{Y}}_g) = \int_{\mathbf{H}_g} P(\mathbf{Y}_g \rightarrow \tilde{\mathbf{Y}}_g, \mathbf{H}_g) \cdot f(\mathbf{H}_g)\, d\mathbf{H}_g \quad (13)$$

where $f(\mathbf{H}_g)$ is the probability density function (PDF) of the effective channel coefficient $\mathbf{H}_g$. Then the analytical ABEP is calculated from the (13) as

$$P_b = \frac{1}{Gp \cdot 2^p} \sum_{g=0}^{G-1} \sum_{\mathbf{Y}_g \in \Lambda} \sum_{\tilde{\mathbf{Y}}_g \in \Lambda, \mathbf{Y}_g \neq \tilde{\mathbf{Y}}_g} P(\mathbf{Y}_g \rightarrow \tilde{\mathbf{Y}}_g) e(\mathbf{Y}_g \rightarrow \tilde{\mathbf{Y}}_g) \quad (14)$$

where $e(\mathbf{Y}_g \rightarrow \tilde{\mathbf{Y}}_g)$ denotes the number of error bits in difference between $\mathbf{Y}_g$ and $\tilde{\mathbf{Y}}_g$.

B. Euclidean Distance Analysis

For an m-element vector set $\mathbf{U}_i = [U_{i,0}, U_{i,1}, \ldots, U_{i,G-1}]^T$ with $i = 0, 1, 2, \ldots, m-1$, the Euclidean distance for any two vectors $\mathbf{U}_i$ and $\mathbf{U}_j$ is represented as $ED(\mathbf{U}_i, \mathbf{U}_j) = \sqrt{\sum_{g=0}^{G-1} |U_{i,g} - U_{j,g}|^2}$. Consequently, the MED in the vector set are calculated by $MED = \min_{i \neq j} ED(\mathbf{U}_i, \mathbf{U}_j)$.

A simplified derivation of MED for SIM symbols before transmitting is given by [3] as

$$MED^t_{IM} = \begin{cases} \frac{2L}{K}, & \text{BPSK } (M=2) \\ \frac{6L}{K(M-1)}, & M-\text{QAM } (M \geq 4) \end{cases}. \quad (15)$$

It apparent from Eq. (15) that the MED becomes larger as the ratio L/K increases. More specifically, upon increasing the sparsity of the symbol vectors, the IM-based systems will improve the reliability of estimating the index bits by enlarging both its MED and AED. Table. 1 provides the MED comparisons between EDCT-OFDM-IM and DFT-OFDM-IM schemes, where MED^t denotes the MED calculated by (15), while MED^p is obtained by simulation with a typical 10-tap Rayleigh Fading channel. It can be observed from Table I that the proposed EDCT-OFDM-IM schemes always have larger MED both in simulation and in theory than that of the DFT-OFDM-IM counterpart at the same SE. This can be explained by the fact that the proposed EDCT-OFDM-IM exhibits larger sparsity than its DFT-OFDM-IM counterpart at the same SE. It should be noted that the simulated MEDs are slightly greater than that of theoretical MED because of the correlation gain as indicated in [12] [13].

C. The CCDF of The PAPR

In the PAPR analysis of this paper, we perform oversampling to approximate its continuous signal. After the IDCT modulation procedure, the time domain symbols within a symbol period is expressed as:

$$s_k = \sum_{n=0}^{\alpha N-1} X_n \beta_n \cos[\frac{\pi n(2k+1)}{2\alpha N}], \quad 0 \leq k \leq \alpha N - 1. \quad (16)$$

where α is the oversampling factor which is an integer larger than 1. PAPR is defined as the ratio of the maximum achievable signal power, P_{max}, and the average signal power, P_{mean}:

$$PAPR = \frac{P_{max}}{P_{mean}} \approx \frac{\max\{|s_k|^2\}}{E\{|s_k|^2\}}. \quad (17)$$

It has been proven that $\alpha = 4$ can achieve fairly accurate PAPR results. The cumulative distribution function (CDF) of the PAPR is commonly employed to illustrate the PAPR performance for a typical system. Alternatively, the complementary CDF (CCDF) [17]-[18] can be used instead of the CDF, which presents the probability that the PAPR within a symbol period exceeds a PAPR threshold. Consequently, the CCDF of the PAPR of a signal data block is derived by

$$P(PAPR > PAPR_0) = 1 - P(PAPR < PAPR_0) \quad (18)$$

.

D. ICI effect Analysis

Considering a normalized carrier frequency offset (CFO) ΔF incurred from the system hardware imperfections, the time

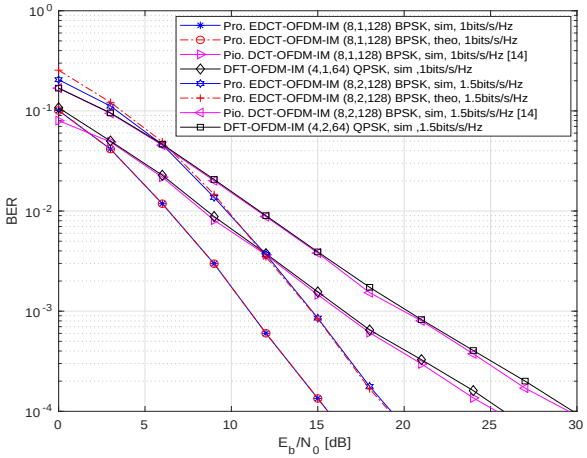

Fig. 1. BER Performance comparison at normalised transmission rate of 1 bits/s/Hz and 1.5 bits/s/Hz.

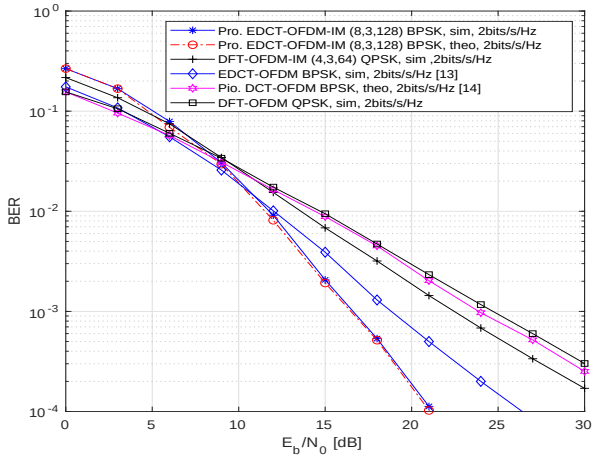

Fig. 2. BER Performance comparison at normalised transmission rate of 2 bits/s/Hz.

domain symbols after IDCT is modified to

$$\tilde{s}_k = \sum_{n=0}^{N-1} X_n \beta_n \cos\left[\frac{\pi(n+\Delta F)(2k+1)}{2N}\right], \quad 0 \le k \le N-1. \tag{19}$$

At the receiver, the received signal at the kth subcarrier provided in (8) is now expressed in the presence of CFO as

$$\tilde{Z}_k = \gamma_{(k,k)} X_k + \underbrace{\sum_{i=0, i\neq k}^{N-1} \gamma_{(i,k)} X_i}_{ICI} + W_k \tag{20}$$

where $\gamma_{(k,k)}$ is the signal power coefficient and W_k is the effective noise in the frequency domain at the kth subcarrier, where $k = 0, 1, 2, \cdots, N-1$. The second term on the right of (20) stands for the overall ICI, where $\gamma_{(i,k)}$ is the ICI coefficient caused by ith subcarrier on the desired kth subcarrier. Specifically, the coefficient $\gamma_{(i,k)}$ is given by:

$$\gamma_{(i,k)} = \beta_i \beta_k \sum_{n=0}^{N-1} \sum_{m=-v}^{N+v-1} \cos\frac{\pi(2m+1)(i+\Delta F)}{2N} \cdot \cos\frac{\pi(2n+1)k}{2N} h(n-m) \tag{21}$$

where $h(n)$ is denoted as the effective channel impulse response in the time domain. The variance of the ICI term on the kth subcarrier is calculated approximately by:

$$N_k^{ICI} = \sum_{i=0, i\neq k}^{N-1} E\{|\gamma_{(i,k)}|^2\} E\{|X_i|^2\} \approx \frac{K}{L} \sum_{i=0, i\neq k}^{N-1} E\{|\gamma_{(i,k)}|^2\}. \tag{22}$$

In this manner, the ICI term and the noise term can be regarded as integrated noise by which the ML detector expressed in (10) can be reformulated to

$$\hat{\mathbf{Y}}_g = \arg\min_{\mathbf{Y}_g \in \Lambda} \sum_{\lambda=0}^{L-1} \frac{|\tilde{Z}_{g+\lambda G} - \gamma_{(g+\lambda G, g+\lambda G)} Y_{g+\lambda G}|^2}{N_k^{ICI} + V_k}. \tag{23}$$

Compared to the traditional DFT-OFDM system, only parts of subcarriers transmitting results in a relative lower signal-to-interference ratio (SIR), hence making the ICI less detrimental on the overall system performance.

IV. Numerical Results

In this section, we present our simulation results for characterizing the achievable performance of our proposed EDCT-OFDM-IM system. We consider a ten-path (i.e. L_c=10) slow-varying Rayleigh fading channel with exponential power delay profile, and the channel information is supposed to be perfectly obtained by the receiver.

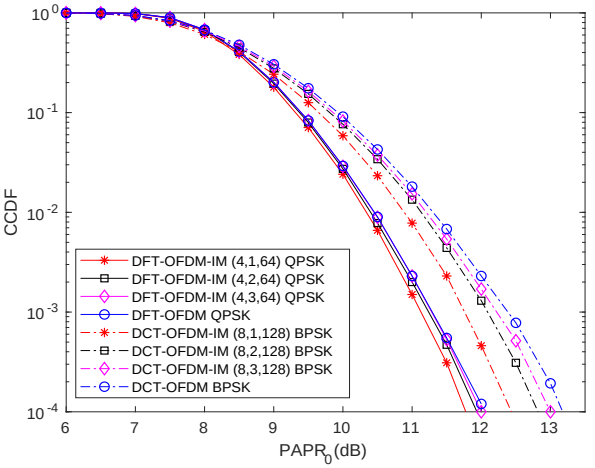

Fig. 3. PAPR performance comparison for classic OFDM, DFT-OFDM-IM and EDCT-OFDM-IM at 2 bits/s/Hz.

Fig. 1 and Fig. 2 compare the BER performance of our proposed EDCT-OFDM-IM to that of DCT-OFDM-IM and DFT-OFDM-IM at normalised transmission rates of 1 bits/s/Hz, 1.5 bits/s/Hz and 2 bits/s/Hz, respectively. The theoretical ABEP of the EDCT-OFDM-IM is added as a benchmarker, which becomes very tight upon increasing the SNR values. It can be seen from Fig. 2 that the proposed EDCT-OFDM-IM with the optimal ML detector is capable of providing significant performance gain over the pioneer assisted DCT-OFDM-IM scheme with linear detector. Moreover, Figs. 1 and 2 show that our proposed EDCT-OFDM-IM scheme outperforms the classic OFDM and OFDM-IM schemes by 10 dB at BER= 10^{-4} in the cases of 1 bits/s/Hz and 2 bits/s/Hz. The superiority in BER performance can be explained by our analytical MED results shown in Table 1. Furthermore, as E_b/N_0 increases, the performance advantages of the EDCT-OFDM-IM schemes becomes more prominent.

As illustrated in Fig. 3, the CCDF of PAPR in DFT-based

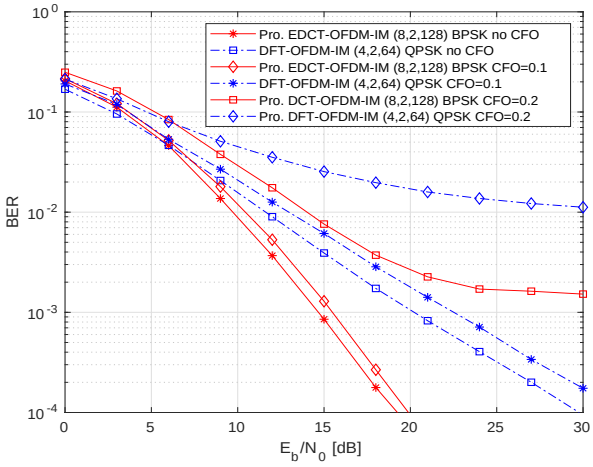

Fig. 4. BER comparison between DFT-OFDM-IM and DCT-OFDM-IM in the presence of CFO at 1.5 bits/s/Hz.

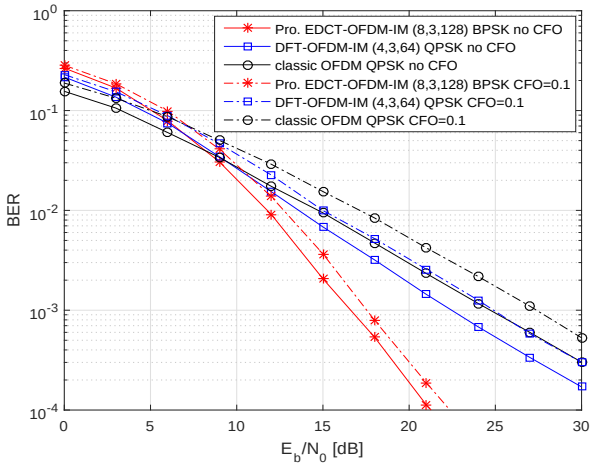

Fig. 5. BER comparison between DFT-OFDM-IM, DCT-OFDM-IM and classic OFDM in the presence of CFO at 2 bits/s/Hz.

schemes performs better than that of DCT-based schemes. This can be explained by the fact that the IFFT size of DFT-OFDM is 64, which is smaller than the IDCT size (128) of the DCT-OFDM at the same bandwidth. The DCT-OFDM-IM schemes exhibit better CCDF performance than its DCT-OFDM counterpart. To be more specific, the DCT-OFDM-IM (8,1,128) outperforms the DCT-OFDM by 1 dB at 10^{-4}.

Finally, Figs. 4 and 5 compare the BER performance of proposed EDCT-OFDM-IM with DFT-OFDM-IM in the context of different CFO values at 2 bits/s/Hz and 1.5 bits/s/Hz, respectively. Moreover, in Fig. 4, the proposed EDCT-OFDM-IM employs (8,3,128) and BPSK, DFT-OFDM-IM employs (4,3,64) and QPSK, as well as OFDM employs QPSK to achieve 2 bits/s/Hz. In Fig. 5, the proposed EDCT-OFDM-IM employs (8,2,128) and BPSK, as well as DFT-OFDM-IM employs (4,2,64) to achieve 1.5 bits/s/Hz. We consider the normalised CFO=0.1 in Fig. 4 and CFO=0.1, 0.2 in Fig. 5. Observe from Figs. 4 and Fig. 5 that the proposed EDCT-OFDM-IM scheme is capable of outperforming the DFT-OFDM-IM and DFT-OFDM schemes by around 10 dB at BER=10^{-3} with CFO=0.1 for both 2 bits/s/Hz and 1.5 bits/s/Hz. It is also shown that the proposed EDCT-OFDM-IM becomes more robust against CFO than the DFT-OFDM-IM and DFT-OFDM counterparts as CFO increases.

V. Conclusion

In this paper, we have illustrated an improved transceiver design for the proposed EDCT-OFDM-IM system and carried out its comparisons with the DFT-OFDM-IM system in terms of several aspects. Through increasing the sparsity of the modulated symbol vector, the associated MED becomes larger without sacrificing throughput. This reveals that the EDCT-OFDM-IM scheme shows an explicit BER advantage than its DFT-based counterpart under the same spectral efficiency. Moreover, we show that the PAPRs of the EDCT-OFDM-IM and the DFT-OFDM-IM systems are almost identical. Furthermore, as the ratio of $(L-K)/L$ is smaller in the DCT-OFDM-IM scheme, it is more robust to ICI effect in the case of high mobility applications. The proposed EDCT-OFDM-IM scheme constitutes a promising solution for some 5G high mobility scenarios, such as V2X communications.

References

[1] E. Basar, M. Wen, et al., "Index modulation techniques for next-generation wireless networks", *IEEE Access*, 2017.

[2] Y. Xiao, S. Wang, et al., "OFDM with interleaved subcarrier-index modulation", *IEEE Communications Letters*, Aug 2014.

[3] N. Ishikawa, S. Sugiura, et al., "Subcarrier-index modulation aided OFDM - will it work?", *IEEE Access*, vol. 4, pp. 2580–2593, 2016.

[4] Lixia Xiao, Bin Xu, et al., "Performance evaluation in PAPR and ICI for ISIM-OFDM systems", in *2014 International Workshop on High Mobility Wireless Communications*, Nov 2014, pp. 84–88.

[5] D. Tsonev, S. Sinanovic, et al., "Enhanced subcarrier index modulation (SIM) OFDM", in *2011 IEEE GLOBECOM Workshops*, Dec 2011.

[6] T. A. Weiss and F. K. Jondral, "Spectrum pooling: an innovative strategy for the enhancement of spectrum efficiency", *IEEE Communications Magazine*, vol. 42, no. 3, pp. S8–14, Mar 2004.

[7] M. Wen, X. Cheng, et al., "Index modulated OFDM for underwater acoustic communications", *IEEE Communications Magazine*, May 2016.

[8] Y. Liu, M. Zhang, H. Wang, et al., "Spatial modulation orthogonal frequency division multiplexing with subcarrier index modulation for v2x communications", in *2016 International Conference on Computing, Networking and Communications (ICNC)*, Feb 2016, pp. 1–5.

[9] G. D. Mandyam, "Sinusoidal transforms in OFDM systems", *IEEE Transactions on Broadcasting*, vol. 50, no. 2, pp. 172–184, June 2004.

[10] W.H Chen et al., "A fast computational algorithm for the discrete cosine transform", *IEEE Transactions on Communications*, vol. 25, no. 9, pp. 1004–1009, Sep 1977.

[11] N. Al-Dhahir et al., "Optimum DCT-based multicarrier transceivers for frequency-selective channels", *IEEE Transactions on Communications*, April 2006.

[12] C. He, L. Zhang, J. Mao, et al., "Performance analysis and optimization of DCT-based multicarrier system on frequency-selective fading channels", *IEEE Access*, vol. 6, pp. 13075–13089, 2018.

[13] C. He, L. Zhang, et al., "Output SNR analysis and detection criteria for optimum DCT-based multicarrier system", in *2016 International Symposium on Wireless Communication Systems*, Sept 2016, pp. 59–64.

[14] M. Chafii, J. P. Coon, et al., "DCT-OFDM with index modulation", *IEEE Communications Letters*, vol. 21, no. 7, pp. 1489–1492, July 2017.

[15] V. Sanchez, P. Garcia, et al., "Diagonalizing properties of the discrete cosine transforms", *IEEE Transactions on Signal Processing*, pp. 2631–2641, Nov 1995.

[16] E. Basar, U. Aygolu, et al., "Orthogonal frequency division multiplexing with index modulation", *IEEE Transactions on Signal Processing*, Nov 2013.

[17] X. Ouyang, J. Jin, G. Jin and Z. Wang, "Low complexity discrete Hartley transform precoded OFDM for peak power reduction", *ELECTRONICS LETTERS* vol. 48 no. 2, 19th January 2012

[18] H. Ochiai and H. Imai, "On the distribution of the peak-to-average power ratio in OFDM signals," *IEEE Trans. Commun.*, vol. 49, no. 2, pp. 282C289, 2001.